Clinical Neurophysiology 132 (2021) 2473–2480

Contents lists available at ScienceDirect

Clinical Neurophysiology

journal homepage: www.elsevier.com/locate/clinph

Alpha-band cortico-cortical phase synchronization is associated with effective connectivity in the motor network

Agnese Zazio [a], Carlo Miniussi [b], Marta Bortoletto [a,*]

[a] Neurophysiology Lab, IRCCS Istituto Centro San Giovanni di Dio Fatebenefratelli, Brescia, BS, Italy
[b] Center for Mind/Brain Sciences – CIMeC, University of Trento, Rovereto, TN, Italy

ARTICLE INFO

Article history:
Accepted 9 June 2021
Available online 30 July 2021

Keywords:
TMS-EEG
Effective connectivity
Weighted phase lag index
Neural oscillations
Communication-through-coherence

HIGHLIGHTS

- Primary motor cortex stimulation triggers early signal transfer to connected regions.
- Pre-stimulus interarea phase synchrony predicts responses in connected brain areas.
- The present data support communication-through-coherence at the macroscale level.

ABSTRACT

Objective: Communication-through-coherence proposes that the phase synchronization (PS) of neural oscillations between cortical areas supports neural communication. In this study, we exploited transcranial magnetic stimulation (TMS)-evoked potentials (TEPs) to test this hypothesis at the macroscale level, i.e., whether PS between cortical areas supports interarea communication. TEPs are electroencephalographic (EEG) responses time-locked to TMS pulses reflecting interarea communication, as they are generated by the transmission of neural activity from the stimulated area to connected regions. If interarea PS is important for communication, it should be associated with the TEP amplitude in the connected areas.

Methods: TMS was delivered over the left primary motor cortex (M1) of fourteen healthy volunteers, and 70-channel EEG was recorded. Early TEP components were source-localized to identify their generators, i.e., distant brain regions activated by M1 through effective connections. Next, linear regressions were used to test the relationship between the TEP amplitude and the pre-stimulus PS between the M1 and the connected regions in four frequency bands (range 4–45 Hz).

Results: Pre-stimulus interarea PS in the alpha-band was positively associated with the amplitude of early TEP components, namely, the N15 (ipsilateral supplementary motor area), P25 (contralateral M1) and P60 (ipsilateral parietal cortex).

Conclusions: Alpha-band PS predicts the response amplitude of the distant brain regions effectively connected to M1.

Significance: Our study supports the role of EEG-PS in interarea communication, as theorized by communication-through-coherence.

1. Introduction

Understanding the mechanisms that underlie neuronal communication within the brain is one of the most intriguing and challenging questions in neuroscience. Although many important features of the pathways of communication and their topological organization have been revealed (Sporns, 2014), little is known about the neurophysiological mechanisms of such communication in the human brain. Therefore, it is fundamental for the future development of connectivity studies to define how brain regions shape effective communication, i.e., directional pathways of interaction that allow the neuronal structure to flexibly exchange signals.

A prominent theory, known as communication-through-coherence (Fries, 2005, 2015), suggests that neural communication is ensured by patterns of coherent neural oscillations, occurring when neural groups oscillate at the same frequency and are phase-locked to each other. This phenomenon is defined as phase

* Corresponding author at: IRCCS Istituto Centro San Giovanni di Dio Fatebenefratelli, Via Pilastroni 4, 25125 Brescia, Italy.
E-mail address: marta.bortoletto@cognitiveneuroscience.it (M. Bortoletto).

https://doi.org/10.1016/j.clinph.2021.06.025
1388-2457/

synchronization (PS). According to the communication-through-coherence framework, PS ensures that temporal windows for neuronal output and input are concurrently open, thus enabling effective communication among pre- and postsynaptic neurons. This exchange takes place via PS, both for small distances within a brain region up to long ranges between distant brain areas (Varela et al., 2001; Schoffelen, 2005). Importantly, the magnitude of the PS, i.e., how much two oscillations are phase-locked to each other, is expected to quantify effective interactions between neural groups.

Most of the evidence supporting the communication-through-coherence framework has been provided at the microscale through intracortical recordings in animals. First, at the local level, it has been shown that the phase of postsynaptic rhythmic activity modulates the input gain and thus effective connectivity. Therefore, the response to any input depends on the oscillatory phase in which they are received so that inputs received at the phase of high excitability of oscillatory activity benefit from a higher gain (Siegle et al., 2014; Ni et al., 2016). Moreover, a second line of evidence comes from the demonstration that the influence of one neural group over another depends on the nonzero PS of the two groups (Womelsdorf et al., 2007; Canolty and Knight, 2010).

Given these premises, it can be assumed that the same mechanisms take place at the macroscale level, i.e., between regions of the human brain, as measured by magneto/electroencephalographic (M/EEG) recordings. Based on this assumption, several studies in the last decade have applied indexes of PS (e.g., imaginary part of coherence, phase locking value, etc.; Bastos and Schoffelen, 2016) to oscillatory M/EEG data as measures of functional connectivity (Stam and van Straaten, 2012; Weisz et al., 2014; Rassi et al., 2019). Nonetheless, to date, noninvasive evidence supporting communication-through-coherence in cortico-cortical communication is limited only to the first line of evidence. In other words, they support the key role of the phase of local oscillations in shaping the neurophysiological and behavioral response to an external event (Thut et al., 2012). In this context, a few studies have exploited transcranial magnetic stimulation (TMS), which has the fundamental advantage of directly activating a cortical area with fine temporal and spatial precision, bypassing the processing pathways of an incoming peripheral stimulus (Miniussi and Thut, 2010). For example, van Elswijk and colleagues (van Elswijk et al., 2010) showed that the amplitude of motor evoked potentials (MEPs) depends on the phase of muscle activity in the beta range at the time of TMS over the motor cortex (van Elswijk et al., 2010). Additionally, the pre-stimulus local alpha phase over the occipital cortex has been shown to be a determinant of visual percepts induced by TMS (e.g., Thut et al., 2011).

Crucially, the role of PS between cortical areas has been less studied in noninvasive recordings, although some evidence has been provided in a recent paper (Stefanou et al., 2018). In this work, TMS was applied either when homologous primary motor cortices (M1s) oscillated in-phase or anti-phase in the alpha-band frequency and the MEPs were recorded in these two conditions. The results showed that interhemispheric inhibition was stronger when alpha oscillations were in-phase between M1s, than when they were in anti-phase. However, PS was studied in a single pathway only (i.e., the interhemispheric connection between M1s) while a cortical area is likely to connect to other regions through multiple pathways at the same time. This has been demonstrated by studies that combined TMS with neuroimaging methods, such as functional magnetic resonance (TMS-fMRI, e.g., Ruff et al., 2009) or EEG (TMS-EEG, e.g., Ilmoniemi et al., 1997). These multimodal approaches play a crucial role in the study of brain connectivity, as they offer the opportunity to draw a causal inference without the application of complex models and assumptions (e.g., dynamic causal modeling and Granger causality). Specifically, TMS-EEG coregistration provides information on the transmission of neural signals with excellent temporal resolution, showing that the activation of a cortical area by means of TMS results in a complex cortical response, including early evoked components generated in several distinct areas (Komssi and Kähkönen, 2006). For example, TMS over M1 activates at least three cortical components in the first 80 ms after the pulse in the TMS-evoked potentials (TEPs) generated through cortico-cortical pathways in addition to activation of the muscles through the corticospinal tract (Komssi et al., 2002). Importantly, the amplitude and latency of the TEP components might reflect, respectively, the strength and conduction delay of the connection between the stimulated area and the receiving area (Bortoletto et al., 2021). In sum, TMS-EEG may be highly informative in the study of cortico-cortical PS in effective connectivity, as it considers multiple complex pathways.

In this study, we aimed to explore the role of PS between cortical areas (i.e., cortico-cortical PS) using a TMS-EEG approach. In this scenario, the target area activated by the TMS represents the presynaptic neural group, and the TEP amplitude induced as a secondary response in distant areas provides the postsynaptic input gain. Next, through EEG, we measured the pre-stimulus PS between the TMS target (i.e., M1) and the regions of secondary responses. Our hypothesis is that effective connectivity, as indexed by the amplitude of TEPs, is related to the nonzero cortico-cortical PS between M1 and the connected regions.

2. Methods

2.1. Participants

Fifteen right-handed healthy volunteers participated in this study, and one was excluded due to excessive muscular artifacts in the EEG recordings. The remaining fourteen volunteers (6 women) were 18–30 years old. The participants had no history of neurological or other relevant medical diseases and had no TMS contraindication (Rossi et al., 2009). None were taking central nervous system-active medication at the time of the recordings. All participants gave their written informed consent and were remunerated for their participation. The experiments were carried out in accordance with the ethical standards of the Declaration of Helsinki and were approved by the local Ethical Committee of IRCCS Istituto Centro San Giovanni di Dio Fatebenefratelli, Brescia, Italy.

2.2. TMS-EEG recording and experimental design

The data analyzed in the present work have been collected as part of a larger study (Veniero et al., 2013). TMS-EEG coregistration of the left M1 area was performed on two separate days with a minimum interval of 48 h (intersession interval, mean ± SE: 3.6 ± 0.5 days) following an identical procedure each day (Fig. 1a). EEG was recorded from 70 sintered scalp electrodes mounted in an elastic cap (BrainCap, Brain Products GmbH, Munich, Germany) according to the international 10–10 system of EEG sensor placement. The FPz electrode was used as the ground electrode, and the TP10 electrode was used as the reference electrode. Horizontal and vertical electrooculograms (EOGs) and electromyograms (EMGs) from the first dorsal interosseous (FDI) were acquired (BrainAmp MRplus, BrainProducts GmbH, Munich, Germany). The skin/electrode impedance was maintained below 5 kΩ. The data were acquired at 5000 Hz and online bandpass filtered between 0.01 and 1000 Hz (Veniero et al., 2009).

Concurrently with the EEG recording, TMS was delivered using a Super Rapid transcranial magnetic stimulator connected to a double 50-mm figure-eight custom coil (Magstim Company, Whitland, UK). The coil was placed tangentially to the scalp with the longer axes perpendicular to the central sulcus, approximately

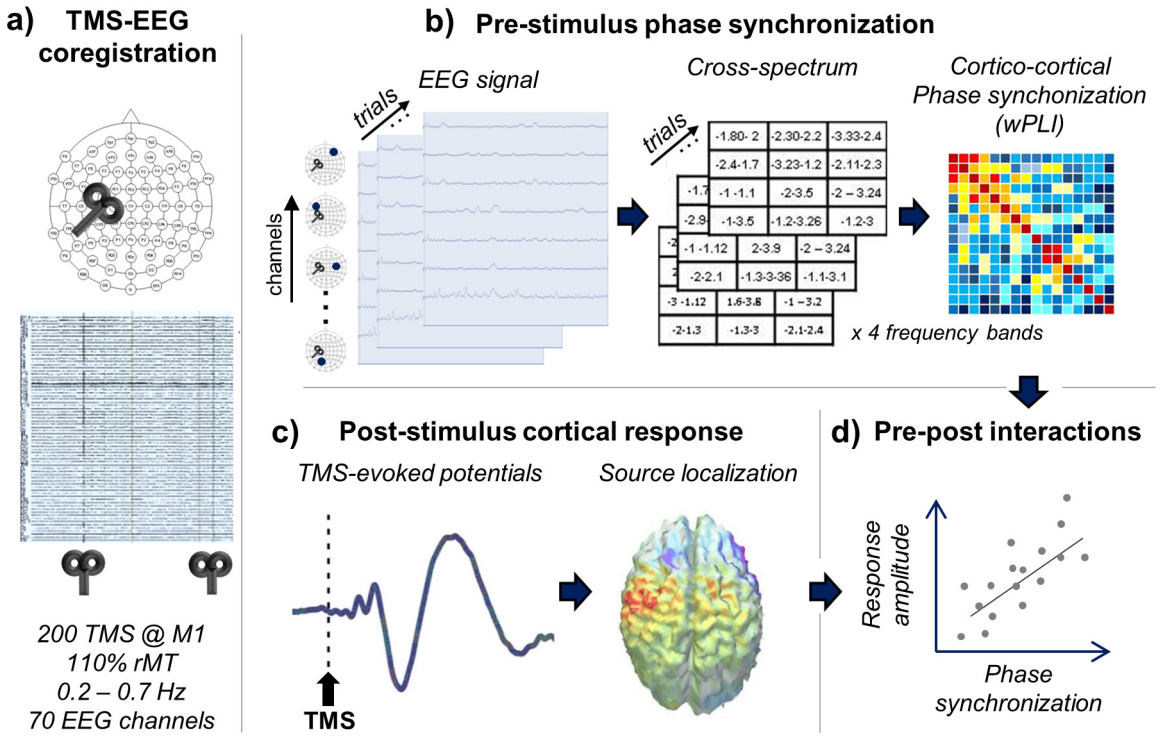

Fig. 1. Schematic of the data acquisition and analysis. a) The experimental procedure of TMS-EEG coregistration included 200 TMS pulses delivered at random frequencies between 1.4 and 5 s (0.2–0.7 Hz) to the left primary motor area (M1) at 110% of the resting motor threshold (rMT), and the EEG was recorded via 70 electrodes. b) Analysis procedure of the pre-stimulus phase synchronization (PS). After preprocessing, the cross-spectrum and weighted phase lag index (wPLI) in the pre-stimulus window were computed for each pair of channels (70 × 70) for four frequency bands (theta, alpha, beta and low gamma). The colors represent coupling strength (red: strongest coupling; dark blue: lowest coupling). c) Analysis procedure of the post-stimulus cortical response. Each TMS-evoked potential (TEP) component was measured by determining the peak value for each subject from the two electrodes that showed the maximum amplitude in the grand average. Then, each component was localized in the cortical space (source localization) by means of standardized low-resolution brain electromagnetic tomography (sLORETA). d) Finally, the relationship between the pre-stimulus wPLI and TEP amplitude was tested by means of simple linear regressions.

45° from the midline. The hotspot for stimulating M1, as identified by eliciting MEPs from the resting right FDI, almost overlapped with the C3 electrode in all subjects. First, the resting motor threshold (rMT) was defined as the TMS intensity that elicited MEPs of at least 50 μV in amplitude in 5 out of 10 trials (mean ± SE: 64.4 ± 1.9% and 63.9% ± 2% of maximal stimulator output; no difference between sessions, $t = 0.9$, $p = 0.39$). Then, 200 single TMS pulses per session were delivered at random intervals between 1.4 and 5 s (i.e., 0.2–0.7 Hz) at 110% of the rMT. The subjects wore earplugs during the entire experiment. The maintenance of the coil position was controlled using a TMS neuronavigation system (SofTaxic, EMS, Bologna, Italy).

2.3. Data analysis

TMS-EEG data analysis was performed in MATLAB (the MathWorks, Natick, MA, USA) with custom scripts using EEGLAB functions (Delorme and Makeig, 2004), FieldTrip functions (Oostenveld et al., 2011), the source-estimate-utilizing noise-discarding (SOUND) algorithm (Mutanen et al., 2018) and the signal-space projection and source-informed reconstruction (SSP-SIR) algorithm (Mutanen et al., 2016).

2.3.1. TMS-EEG preprocessing

The TMS-induced artifact, typically lasting up to 5 ms with our equipment (Veniero et al., 2009), was removed by interpolating the signal from −2 to 5 ms by replacing the artifact signal with a moving average of 5 points starting from 4 ms before the TMS pulse. Then, the EEG and EOG signals were high-pass filtered at 0.1 Hz (zero-phase Butterworth filter), divided into epochs from −1100 ms to 500 ms, baseline corrected based on the 500 ms period before the TMS (from −502 to −2 ms) and reduced to the 2048 sampling rate to speed up signal processing while keeping a high temporal resolution, as required for the TMS-EEG data analysis. To further reduce the TMS-EEG artifacts, the following steps were performed: the measurement noise was reduced with the SOUND algorithm, applied with the same parameters as in the original work (Mutanen et al., 2018); the remaining noisy trials were removed by visual inspection; ocular artifacts were corrected with infomax independent component analysis (ICA); and TMS-evoked muscular artifacts were reduced with the SSP-SIR algorithm (Mutanen et al., 2016) applied to the first 50 ms after the TMS pulse. Muscle-artifact components (0–3 in each dataset) were identified from the time–frequency pattern and the corresponding signal power. The use of SOUND and SSP-SIR algorithms to discard TMS-related artifacts while preserving TMS-related cortical activity was chosen, as these algorithms do not rely on the assumption that neural signals and artifacts are independent and they have been applied by several research groups (Bagattini et al., 2019; Bortoletto et al., 2021; Mancuso et al., 2021; Rogasch et al., 2020; Salo et al., 2019). Finally, the epochs were low-pass filtered at 70 Hz, re-referenced to the average reference and visually inspected to reject noisy trials. No channels were removed or interpolated. For consistency with the analysis on pre-stimulus cortico-cortical PS, the same number of epochs was considered for each participant (25% of trials rejected; see the next paragraph).

2.3.2. Prestimulus cortico-cortical PS

Cortico-cortical PS in the pre-stimulus interval was estimated by calculating the weighted phase lag index (wPLI) (as in Vinck et al., 2011) on the cross-spectrum of the 1000 ms preceding the TMS pulse (Fig. 1b) (fast Fourier transform; Hanning window; fre-

quency resolution = 1 Hz) for each pair of EEG channels and in a range of frequencies from 4 to 45 Hz (theta, alpha, beta and low gamma). Crucially, to obtain an accurate estimation of pre-stimulus PS, the wPLI was calculated after merging trials from the two recording sessions to increase the accuracy (see the Statistical analysis and Results section) and using exactly the same number of EEG epochs (i.e., 339) for each subject to avoid any confounds related to different amounts of data (Bastos and Schoffelen, 2016). The obtained wPLI was then averaged over the following frequency bands: theta (4–7 Hz), alpha (8–13 Hz), beta (14–30 Hz), and low gamma (31–45 Hz), and the absolute value was calculated. Given that the wPLI is a lagged measure of connectivity based solely on the imaginary part of the cross-spectrum and that it performs well in the presence of noise (Vinck et al., 2011), our approach provided a measure of PS that is unbiased and is only minimally affected by volume conduction (Yu, 2020). In subsequent analysis, the high dimensionality of the PS data (i.e., 70x70 electrode pairs) was reduced by focusing on wPLI between the stimulated site (i.e., C3) and the electrodes in which the TEP component was found to be maximal (see next paragraph). In this way, we were able to restrict our pre-stimulus PS analysis to the brain areas connected to M1 that were involved in signal propagation during the first 60 ms following the TMS pulse.

2.3.3. Poststimulus effective connectivity

Given that TMS-EEG allows us to record the propagation of cortical activation from the stimulated area to the connected areas, we exploited TEPs as a measure of effective connectivity. TEPs were analyzed in the same 339 epochs considered in the PS analyses (Fig. 1c). The EEG epochs were baseline-corrected from −100 to −2 ms before the TMS and averaged. From the grand average, we individuated three TEP components within the first 60 ms following the TMS pulse; later components were not considered because they are likely to be contaminated by sensory processing of the TMS pulse (i.e., auditory and somatosensory processing; Nikouline et al., 1999; Herring et al., 2015; please see Figure S1 for further information on sensory contamination). For each component and each subject, we identified the peak value from the mean of the two electrodes that showed the maximum amplitude in the grand average and measured the mean amplitude of 10 ms around the peak.

2.3.4. Cortical sources localization

From previous studies (Ilmoniemi et al., 1997; Komssi et al., 2002; Momi et al., 2021), we expected the TEPs to reflect the diffusion of neural activity to the interconnected brain regions rather than being a local phenomenon confined to the stimulated area, i.e., M1. To identify the cortical regions connected to M1, we localized the cortical sources of each component by calculating the current density distribution at 6,239 voxels (5 mm resolution) at the time of the peak by means of standardized low-resolution brain electromagnetic tomography (sLORETA) (Pascual-Marqui, 2002). Cortical source localization was performed on grand average data across all participants to increase the signal-to-noise ratio. A regularization parameter of the signal-to-noise ratio = 10 was applied to account for residual noise in the signal (Liu et al., 2002). Brain coordinates of the maximal activations are reported according to the Montreal Neurological Institute (MNI) space.

2.4. Statistical analysis

Before merging the trials of the two TMS-EEG sessions, to estimate the variability across recording sessions, TEPs obtained from the first session were compared to TEPs obtained in the second session by means of two-tailed paired *t*-tests applied to the peak amplitude of each component. Furthermore, TEPs from the two sessions were also compared by means of a nonparametric cluster-based permutation test for dependent samples (two-tailed t-statistics, approximated with a Monte Carlo procedure using 1000 permutations; Maris and Oostenveld, 2007) over all channels and time points from 100 ms before to 400 ms after the TMS pulse. Finally, as a measure of test–retest reliability, we calculated the concordance correlation coefficient (CCC) on peak amplitude (Lin, 1989), and the obtained values were interpreted according to (Shrout, 1998).

As a final and key point, the relationship between pre-stimulus cortico-cortical PS (pre-stimulus wPLI) and effective connectivity (indexed by TEPs amplitude) was tested by single linear regressions for each frequency band and TEP component separately.

Statistical significance was set at $p < 0.05$, and all analyses were performed in R software (R Core Team, 2013).

3. Results

3.1. Poststimulus effective connectivity

The first step was to ascertain the response induced by TMS over M1. The comparison between the peak amplitudes in the two separated sessions as well as the cluster-based permutation test over channels and time points confirmed that the TEPs were not different between sessions (paired t-test on TEP peaks: N15: t = -1.2, p = 0.24; P25: t = 1.7, p = 0.12; P60: t = 1, p = 0.34; cluster-based analysis: cluster-corrected $p > 0.29$). Moreover, CCC indicated moderate test–retest reliability between sessions for the N15 amplitude (CCC = 0.73) and substantial reliability for both the P25 (CCC = 0.82) and P60 amplitude (CCC = 0.81) (Lin, 1989; Shrout, 1998). These results showed that overall, the induced response was stable over the sessions; therefore, trials from the two sessions were merged together in subsequent analyses to obtain a reliable number of trials for PS calculation.

Importantly, we analyzed the diffusion of cortical activation after the TMS pulse by localizing the TEP components in the source space to identify brain regions effectively connected with M1. Our results showed that cortical activation induced by TMS within the first 60 ms was not limited to the primary response of the stimulated left M1 area. The induced activation was relayed to a network of regions, generating a series of TEPs secondary to the activation of the target area (M1), including the N15 (CP3), P25 (FC2 and C2) and P60 (CP3 and CP5) waveforms (Fig. 2 and Fig. 3b). For the P25 and P60 components, wPLI was averaged over the two electrode pairs that were considered (C3-FC2 and C3-C2 for P25; C3-CP3 and C3-CP5 for P60), as reported in Fig. 3a. The source localization of the TEPs revealed that these components were generated within the motor and parietal cortices: N15 was localized in the left supplementary motor area (SMA, left Brodmann area (BA) 6; MNI coordinates: −5, −10, 55); P25 was localized in the contralateral M1 (right BA4; MNI coordinates: 5, −20, 60); and the positive deflection corresponding to P60 was localized in the left superior parietal lobule (left BA7; MNI coordinates: −25, −60, 50) (Fig. 2 lower panel). Overall, our results on source localization are in line with previous evidence characterizing TEPs as nonlocal phenomena that reflect the transmission of neural activation to interconnected brain regions and therefore can be considered a measure of effective connectivity.

3.2. Relationship between the pre-stimulus cortico-cortical PS and effective connectivity

The second and significant step was to identify whether there was a relationship between the cortico-cortical PS before TMS (pre-stimulus wPLI) and effective connectivity (TEP amplitude).

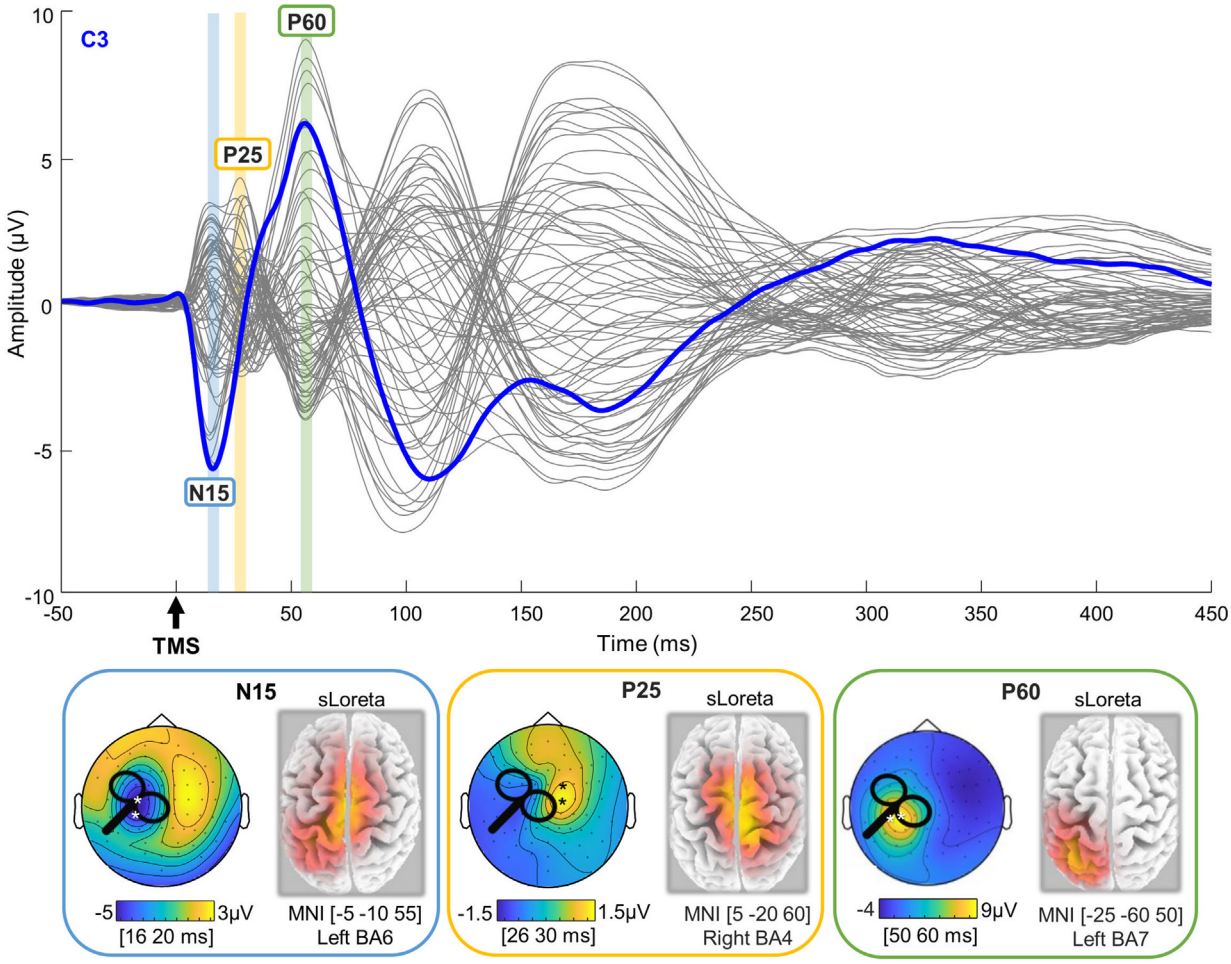

Fig. 2. TMS-evoked potentials: TEP components within 60 ms (N15, P25 and P60) were identified on the scalp and localized in the source space. *Top:* Butterfly plot of TEPs across 70 EEG scalp channels in average reference; C3 electrode in the thick blue trace. *Bottom*: topographies and source localization of TEP components; maximum activation is indicated by Montreal Neurological Institute (MNI) coordinates and the corresponding Brodmann area (BA). After the activation of the M1 target area, several other cortical regions were activated at different latencies: N15 localized in the left supplementary motor area (BA6), P25 in the right precentral gyrus (BA4), and P60 in the left superior parietal lobule (BA7).

We observed a significant positive relationship between C3 pre-stimulus wPLI in the alpha band and three TEP components, such that subjects with stronger connections in the alpha band between the stimulated area and the connected areas exhibited larger TEP responses (N15: r = -0.54, p = 0.046; P25: r = 0.56, p = 0.036; P60: r = 0.66, p = 0.01), as reported in Fig. 3. No significant relationships were observed between the TEPs amplitude and pre-stimulus cortico-cortical PS in the other frequency bands (see Table S1).

4. Discussion

In the present work, we showed that PS between brain areas could account for effective connectivity, indexed by the amplitude of the cortical response in distant brain regions. Specifically, in the propagation of the signal following M1-TMS, TMS-induced secondary responses were localized in brain areas within the motor and parietal areas, and their response amplitude depended on the strength of the alpha-band PS between these areas and M1 before the TMS pulse.

As expected, we reported evidence that TMS over M1 triggers multiple pathways of cortical activations within the first 60 ms, as revealed by source localization of the TEP components. After M1 stimulation, the signal propagates ipsilaterally to the SMA (N15), to the contralateral homologous M1 (P25), and to the ipsilateral superior parietal lobule (P60). This pattern of brain activation following the TMS pulse is consistent with previous findings on M1 stimulation during resting-state TMS-EEG recording (Ilmoniemi et al., 1997; Komssi et al., 2002; Litvak et al., 2007). Notably, the observation of neural activity in the contralateral hemisphere at ~20 ms after the TMS pulse, together with previous TMS-EEG studies (Ilmoniemi et al., 1997; Komssi et al., 2002; Bortoletto et al., 2021), converges in indicating the time range of ~20 ms as the transcallosal conduction delay between homologous M1s (although shorter latencies have been reported with double-coil TMS studies; e.g., Ferbert et al., 1992; Fujiyama et al., 2016). Moreover, these secondary responses were mainly generated in a network of areas that, according to fMRI studies, are strongly connected during the resting state and have been identified as the motor network (Smith et al., 2009; Patriat et al., 2013). Additionally, activation of the superior parietal lobule following M1 stimulation has been previously reported (Komssi et al., 2002). Importantly, by considering TEP components within the first 60 ms after the TMS pulse, we minimized the risk of sensory contamination (Nikouline et al., 1999; Herring et al., 2019; Niessen et al., 2021; Rocchi et al., 2021; but see Conde et al., 2019). This has been confirmed by additional analyses based on the approach suggested by Niessen and colleagues (Niessen et al.,

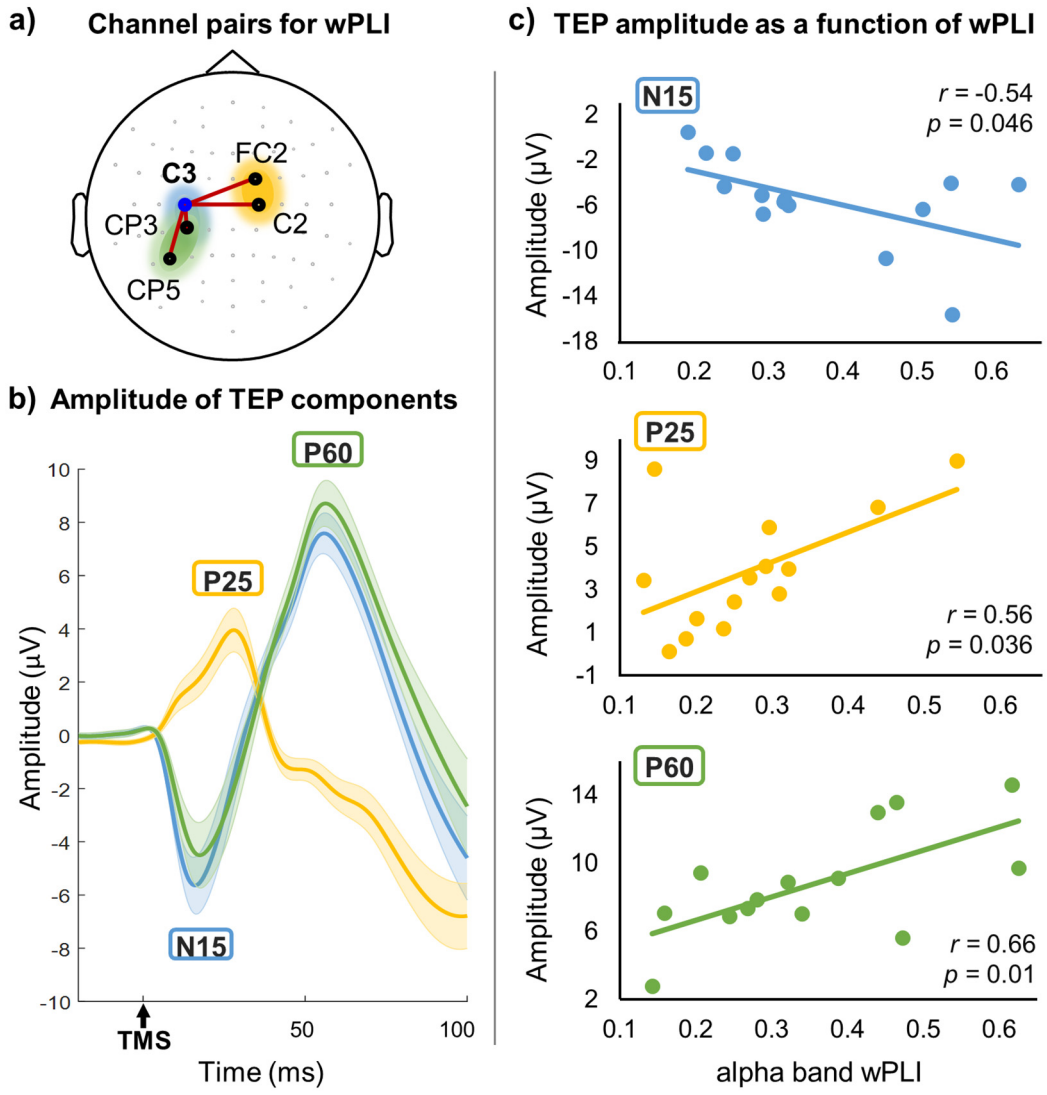

Fig. 3. Relationship between pre-stimulus weighted phase lag index (wPLI) and TMS-evoked potential (TEP) amplitude. a) Pre-stimulus wPLI was calculated between the C3 and electrodes showing the highest peak in TEPs (CP3 for N15, FC2 and C2 for P25, CP3 and CP5 for P60). b) Grand average of TEP components averaged over the electrodes specified in a); standard error for repeated measures (Morey, 2008) in shaded error bars. c) Stronger pre-stimulus connectivity in the alpha band predicts higher TEPs, as shown by significant regressions for all TEP components (N15, P25 and P60).

2021; Figure S1). Considering that we stimulated M1, TEPs within this time interval may be influenced by the reafferent signal of the MEPs; however, this should not be considered contamination but rather as a signal contribution from the stimulated corticospinal circuit.

Overall, the brain source localization of EEG responses to TMS corroborates the common interpretation that TEPs convey information on effective connectivity within a neural network (Bortoletto et al., 2015).

Crucially, we showed that alpha-band PS between M1 and connected regions positively predicts the amplitude of the cortical response to TMS, such that the stronger the functional connectivity is, the greater the cortical response of areas connected to M1 after stimulation.

Our findings advocate the key role of the oscillatory phase in neural communication (Fries, 2005, 2015) by showing that the TMS cortical response is influenced by the preceding PS between the sending region and the region that receives the information, expanding on previous evidence from invasive recordings (Womelsdorf et al., 2007). A possible mechanism behind communication-through-coherence was proposed in a previous animal study (Canolty et al., 2010), which revealed that oscillatory phase coupling across multiple brain areas could selectively synchronize neuronal groups and determine spike timing in single neurons. Neuronal spiking was effectively predicted by the phase-coupling pattern with given distant areas, suggesting that brain oscillations and their interactions are crucial in establishing large-scale brain networks by way of phase coupling across sites. Our results provide stimulating novel evidence consistent with communication-through-coherence predictions at the macroscale in the living human brain; namely, PS is related to the input gain in interarea neural communication in multiple parallel pathways. The significant relationship between alpha-band PS and the amplitude of the response to TMS is not only in line with recent work by Stefanou et al., 2018 but also further extends their results from the peripheral (i.e., MEPs in Stefanou et al., 2018) to the cortical level of the response (i.e., TEPs in the present work) and from a single (i.e., communication between homologous M1s in Stefanou et al., 2018) to multiple parallel pathways within the motor network. Importantly, our data are in line with the most recent conceptualization

of communication-through-coherence (Fries, 2015), in which phase delays have been accounted for, as the estimation of the PS in our study by means of wPLI is relatively insensitive to phase differences of 0° and 180° and therefore implies a delay in the phase (Bastos and Schoffelen, 2016). Overall, the present findings support the use of M/EEG-PS as a measure of interarea connectivity (Weisz et al., 2014; Bastos and Schoffelen, 2016), which so far has been mostly based on the communication-through-coherence hypothesis (Fries, 2005, 2015) and evidence from invasive microscale recordings (Womelsdorf et al., 2007; Canolty et al., 2010).

In relation to the frequency at which the effects were found, PS appears to be predictive of TEP amplitude in the alpha-band only. This result is consistent with a key role played by the alpha-band in the motor system (Haegens et al., 2011), which is also known as mu rhythm and appears to be prominent at rest (Hari, 2006; Ramos-Murguialday and Birbaumer, 2015), specifically in establishing interarea communication (Stefanou et al., 2018). In addition to the alpha rhythm, other frequencies have been associated with activity in the motor system, such as the beta- and gamma-bands; nonetheless, these rhythms appear to be mostly involved during peripheral control or during task execution (Wiesman et al., 2020; Zhang et al., 2020). Therefore, we do not exclude that in a different context than the one investigated here (i.e., the resting state), PS in frequencies other than the alpha-band may be predictive of the response amplitude.

Our study does have a few limitations. First, although we minimized the risk of sensory contamination by focusing on the earliest TEP components within the first 60 ms, N15 showed a trend for significance in the correlation with the rMT, indicating that N15 may contain residual TMS artifacts. Additionally, considering that the test–retest reliability of N15 was lower than that of the other components according to the CCC (i.e., moderate vs. substantial reliability), additional caution should be used during the interpretation of the results from this component. Second, the relatively small sample size, although consistent with TMS-EEG studies recently published (Koivisto et al., 2017; Gordon et al., 2018; Pisoni et al., 2018; Stefanou et al., 2018; Conde et al., 2019), restricts the generalization that can be drawn from the results, which therefore must be interpreted with caution until future studies provide a replication of the results. Third, neither wPLI nor TEPs can be obtained at the single-trial level, thus preventing the study of within-subject fluctuations in effective connectivity and the response to TMS. Finally, we highlight that while the present data show an association between pre-stimulus PS and TEP amplitude, they do not demonstrate a causal effect and, therefore, should not be interpreted in this sense.

In conclusion, our findings highlight the role of EEG oscillations in creating pathways of communication in functional brain networks. Importantly, we provide valuable macroscale evidence supporting the communication-through-coherence framework in the communication between distinct areas, indicating PS as a promising neurophysiological mechanism through which effective communication between cortical regions is organized.

5. Data availability statement

Raw TMS-EEG data are openly available at: https://gin.g-node.org/AgneseZazio/ZazioMiniussiBortoletto2021

Declaration of Competing Interest

The authors declare that they have no known competing financial interests or personal relationships that could have appeared to influence the work reported in this paper.

Acknowledgments

We thank Domenica Veniero for her help with data collection, Clarissa Ferrari for her assistance with statistical analyses and Tuomas P. Mutanen for providing the codes for the SOUND and SSP-SIR algorithms used in the TMS-EEG preprocessing. This work was supported by the Italian Ministry of Health Funding - 'Ricerca Corrente'.

Appendix A. Supplementary material

Supplementary data to this article can be found online at https://doi.org/10.1016/j.clinph.2021.06.025.

References

Bagattini C, Mutanen TP, Fracassi C, Manenti R, Cotelli M, Ilmoniemi RJ, et al. Predicting Alzheimer's disease severity by means of TMS–EEG coregistration. Neurobiol Aging 2019;80:38–45.
Bastos AM, Schoffelen J-M. A Tutorial Review of Functional Connectivity Analysis Methods and Their Interpretational Pitfalls. Front Syst Neurosci 2016;9:175.
Bortoletto M, Bonzano L, Zazio A, Ferrari C, Pedullà L, Gasparotti R, et al. Asymmetric transcallosal conduction delay leads to finer bimanual coordination. Brain Stimul 2021;14(2):379–88.
Bortoletto M, Veniero D, Thut G, Miniussi C. The contribution of TMS – EEG coregistration in the exploration of the human cortical connectome. Neurosci Biobehav Rev 2015;49:114–24.
Canolty RT, Ganguly K, Kennerley SW, Cadieu CF, Koepsell K, Wallis JD, et al. Oscillatory phase coupling coordinates anatomically dispersed functional cell assemblies. PNAS 2010;107(40):17356–61.
Canolty RT, Knight RT. The functional role of cross-frequency coupling. Trends Cogn Sci 2010;14:506–15.
Conde V, Tomasevic L, Akopian I, Stanek K, Saturnino GB, Thielscher A, et al. The nontranscranial TMS-evoked potential is an inherent source of ambiguity in TMS-EEG studies. Neuroimage 2019;185:300–12.
Ferbert A, Priori A, Rothwell JC, Day BL, Colebatchi JG, Marsden CD. Interhemispheric Inhibition of the Human Motor Cortex. J Physiol 1992;453:525–46.
Fries P. A mechanism for cognitive dynamics: Neuronal communication through neuronal coherence. Trends Cogn Sci 2005;9(10):474–80.
Fries P. Rhythms for Cognition: Communication through Coherence. Neuron 2015;88:220–35.
Fujiyama H, Van Soom J, Rens G, Gooijers J, Leunissen I, Levin O, et al. Age-Related Changes in Frontal Network Structural and Functional Connectivity in Relation to Bimanual Movement Control. J Neurosci 2016;36(6):1808–22.
Gordon PC, Desideri D, Belardinelli P, Zrenner C, Ziemann U. Brain Stimulation Comparison of cortical EEG responses to realistic sham versus real TMS of human motor cortex. Brain Stimul 2018;11:1322–30.
Haegens S, Nacher V, Luna R, Romo R, Jensen O. α-Oscillations in the monkey sensorimotor network influence discrimination performance by rhythmical inhibition of neuronal spiking. PNAS 2011;108:19377–82.
Hari R. Action-perception connection and the cortical mu rhythm. Prog Brain Res 2006;159:253–60.
Herring JD, Esterer S, Marshall TR, Jensen O, Bergmann TO. Low-frequency alternating current stimulation rhythmically suppresses gamma-band oscillations and impairs perceptual performance. Neuroimage 2019;184:440–9.
Herring JD, Thut G, Jensen O, Bergmann TO. Attention Modulates TMS-Locked Alpha Oscillations in the Visual Cortex. J Neurosci 2015;35:14435–47.
Ilmoniemi RJ, Virtanen J, Ruohonen J, Karhu J, Aronen HJ, Näätänen R, et al. Neuronal responses to magnetic stimulation reveal cortical reactivity and connectivity. NeuroReport 1997;8(16):3537–40.
Koivisto M, Grassini S, Hurme M, Salminen-Vaparanta N, Railo H, Vorobyev V, et al. TMS-EEG reveals hemispheric asymmetries in top-down influences of posterior intraparietal cortex on behavior and visual event-related potentials. Neuropsychologia 2017;107:94–101.
Komssi S, Aronen HJ, Huttunen J, Kesäniemi M, Soinne L, Nikouline VV, et al. Ipsi- and contralateral EEG reactions to transcranial magnetic stimulation. Clin Neurophysiol 2002;113(2):175–84.
Komssi S, Kähkönen S. The novelty value of the combined use of electroencephalography and transcranial magnetic stimulation for neuroscience research. Brain Res Rev 2006;52(1):183–92.
Lin L-K. A Concordance Correlation Coefficient to Evaluate Reproducibility. Biometrics 1989;45(1):255.
Litvak V, Komssi S, Scherg M, Hoechstetter K, Classen J, Zaaroor M, et al. Artifact correction and source analysis of early electroencephalographic responses evoked by transcranial magnetic stimulation over primary motor cortex. Neuroimage. 2007;37(1):56–70.
Liu AK, Dale AM, Belliveau JW. Monte Carlo simulation studies of EEG and MEG localization accuracy. Hum Brain Mapp 2002;16(1):47–62.

Mancuso M, Sveva V, Cruciani A, Brown K, Ibáñez J, Rawji V, et al. Transcranial Evoked Potentials Can Be Reliably Recorded with Active Electrodes. Brain Sci 2021;11(2):145.
Maris E, Oostenveld R. Nonparametric statistical testing of EEG- and MEG-data. J Neurosci Methods 2007;164(1):177–90.
Miniussi C, Thut G. Combining TMS and EEG offers new prospects in cognitive neuroscience. Brain Topogr 2010;22(4):249–56.
Momi D, Ozdemir RA, Tadayon E, Boucher P, Shafi MM, Pascual-Leone A, et al. Network-level macroscale structural connectivity predicts propagation of transcranial magnetic stimulation. Neuroimage 2021;229:117698.
Morey. Confidence intervals from normalized data: a correction to Cosineau (2005). Tutorial in Quantitative Methods for Psychology 2008;4(2):61–4.
Mutanen TP, Kukkonen M, Nieminen JO, Stenroos M, Sarvas J, Ilmoniemi RJ. Recovering TMS-evoked EEG responses masked by muscle artifacts. Neuroimage 2016;139:157–66.
Mutanen TP, Metsomaa J, Liljander S, Ilmoniemi RJ. Automatic and robust noise suppression in EEG and MEG: The SOUND algorithm. Neuroimage 2018;166:135–51.
Ni J, Wunderle T, Lewis CM, Desimone R, Diester I, Fries P. Gamma-Rhythmic Gain Modulation. Neuron 2016;92:240–51.
Niessen E, Bracco M, Mutanen TP, Robertson EM. An analytical approach to identify indirect multisensory cortical activations elicited by TMS? Brain Stimul 2021;14(2):376–8.
Nikouline V, Ruohonen J, Ilmoniemi RJ. The role of the coil click in TMS assessed with simultaneous EEG. Clin Neurophysiol 1999;110(8):1325–8.
Oostenveld R, Fries P, Maris E, Schoffelen J-M. FieldTrip: Open source software for advanced analysis of MEG, EEG, and invasive electrophysiological data. Comput Intell Neurosci 2011:1–9.
Patriat R, Molloy EK, Meier TB, Kirk GR, Nair VA, Meyerand ME, et al. The effect of resting condition on resting-state fMRI reliability and consistency: A comparison between resting with eyes open, closed, and fixated. Neuroimage 2013;78:463–73.
Pascual-Marqui RD. Standardized low-resolution brain electromagnetic tomography (sLORETA): technical details. Methods Find. Exp. Clin. Pharmacol. 2002;24:5–12.
Pisoni A, Romero Lauro L, Vergallito A, Maddaluno O, Bolognini N. Cortical dynamics underpinning the self-other distinction of touch: A TMS-EEG study. Neuroimage 2018;178:475–84.
R Core Team. A language and environment for statistical computing. R Foundation for Statistical Computing, Vienna, Austria 2013. https://www.r-project.org.
Ramos-Murguialday A, Birbaumer N. Brain oscillatory signatures of motor tasks. J Neurophysiol 2015;113(10):3663–82.
Rassi E, Wutz A, Müller-Voggel N, Weisz N. Prestimulus feedback connectivity biases the content of visual experiences. PNAS 2019;116(32):16056–61.
Rocchi L, Di Santo A, Brown K, Ibáñez J, Casula E, Rawji V, et al. Disentangling EEG responses to TMS due to cortical and peripheral activations. Brain Stimul 2021;14(1):4–18.
Rogasch NC, Zipser C, Darmani G, Mutanen TP, Biabani M, Zrenner C, et al. The effects of NMDA receptor blockade on TMS-evoked EEG potentials from prefrontal and parietal cortex. Sci Rep 2020;10(1).
Rossi S, Hallett M, Rossini PM, Pascual-Leone A. Safety of TMS Consensus Group. Safety, ethical considerations, and application guidelines for the use of transcranial magnetic stimulation in clinical practice and research. Clin Neurophysiol 2009;120(12):2008–39.
Ruff CC, Driver J, Bestmann S. Combining TMS and fMRI: From "virtual lesions" to functional-network accounts of cognition. Cortex 2009;45:1043–9.
Salo KS-T, Mutanen TP, Vaalto SMI, Ilmoniemi RJ EEG. Artifact Removal in TMS Studies of Cortical Speech Areas. Brain Topogr 2019:33.
Schoffelen J-M. Neuronal coherence as a mechanism of effective corticospinal interaction. Science 2005;308(5718):111–3.
Shrout PE. Measurement reliability and agreement in psychiatry. Stat Methods Med Res 1998;7(3):301–17.
Siegle JH, Pritchett DL, Moore CI. Gamma-range synchronization of fast-spiking interneurons can enhance detection of tactile stimuli. Nat Neurosci 2014;17(10):1371–9.
Smith SM, Fox PT, Miller KL, Glahn DC, Fox PM, Mackay CE, et al. Correspondence of the brain's functional architecture during activation and rest. PNAS 2009;106(31):13040–5.
Sporns O. Contributions and challenges for network models in cognitive neuroscience. Nat Neurosci 2014;17(5):652–60.
Stam CJ, van Straaten ECW. The organization of physiological brain networks. Clin Neurophysiol 2012;123:1067–87.
Stefanou MI, Desideri D, Belardinelli P, Zrenner C, Ziemann U. Phase synchronicity of μ-rhythm determines efficacy of interhemispheric communication between human motor cortices. J Neurosci 2018;38:10525–34.
Thut G, Miniussi C, Gross J. The functional importance of rhythmic activity in the brain. Curr Biol 2012;22:R658–63.
Thut G, Veniero D, Romei V, Miniussi C, Schyns P, Gross J. Rhythmic TMS causes local entrainment of natural oscillatory signatures. Curr Biol 2011;21:1176–85.
Delorme A, Makeig S. EEGLAB: an open source toolbox for analysis of single-trial EEG dynamics including independent component analysis. J Neurosci Methods 2004;134:9–21.
van Elswijk G, Maij F, Schoffelen J-M, Overeem S, Stegeman DF, Fries P. Corticospinal beta-band synchronization entails rhythmic gain modulation. J Neurosci 2010;30(12):4481–8.
Varela F, Lachaux JP, Rodriguez E, Martinerie J. The brainweb: phase synchronization and large-scale integration. Nat Rev Neurosci 2001;2:229–39.
Veniero D, Bortoletto M, Miniussi C. TMS-EEG coregistration: On TMS-induced artifact. Clin Neurophysiol 2009;120:1392–9.
Veniero D, Bortoletto M, Miniussi C. Cortical modulation of short-latency TMS-evoked potentials. Front Hum Neurosci 2013;6:1–7.
Vinck M, Oostenveld R, van Wingerden M, Battaglia F, Pennartz CMA. An improved index of phase-synchronization for electrophysiological data in the presence of volume-conduction, noise and sample-size bias. Neuroimage 2011;55(4):1548–65.
Weisz N, Wühle A, Monittola G, Demarchi G, Frey J, Popov T, et al. Prestimulus oscillatory power and connectivity patterns predispose conscious somatosensory perception. PNAS 2014;111:417–25.
Wiesman AI, Koshy SM, Heinrichs-Graham E, Wilson TW. Beta and gamma oscillations index cognitive interference effects across a distributed motor network. Neuroimage 2020;213:116747.
Womelsdorf T, Schoffelen J-M, Oostenveld R, Singer W, Desimone R, Engel AK, et al. Modulation of neuronal interactions through neuronal synchronization. Science 2007;316(5831):1609–12.
Yu M. Benchmarking metrics for inferring functional connectivity from multichannel EEG and MEG: A simulation study. Chaos. 2020;30(12):123124.
Zhang X, Li H, Xie T, Liu Y, Chen J, Long J. Movement Speed Effects on Beta-band Oscillations in Sensorimotor Cortex during Voluntary Activity. J Neurophysiol 2020;124(2):352–9.